

# Electronic Supplementary information

## On the activation of PhICl<sub>2</sub> with pyridine

Tiffany B. Poynder,<sup>a</sup> Analia I. Chamorro Orué<sup>b</sup>, Tania,<sup>a</sup> Lachlan Sharp-Bucknall,<sup>a</sup> Matthew T. Flynn,<sup>a</sup> David J. D. Wilson<sup>a</sup>, , Kasun Sankalpa Athukorala Arachchige<sup>b</sup>, Jack K. Clegg<sup>b\*</sup> and Jason L. Dutton<sup>a\*</sup>

<sup>a</sup>Department of Chemistry and Physics, La Trobe University, Melbourne, Victoria, Australia

<sup>b</sup>School of Chemistry and Molecular Biosciences, The University of Queensland, St Lucia, Queensland 4072,

j.clegg@uq.edu.au, j.dutton@latrobe.edu.au

### Table of Contents

1.	Experimental methods .....	2
1.1.	Synthesis and crystallisation .....	2
2.	Data collection and details of structure refinement .....	3
2.1.	Multipole modelling of 1 .....	4
2.2.	Topological analysis .....	4
3.	NMR Investigations.....	8
4.	Computational details .....	23
5.	References .....	26

## 1. Experimental methods

### 1.1. Synthesis and crystallisation

#### Preparation of Iodobenzene dichloride ( $\text{PhCl}_2$ )

Concentrated HCl (10 mL, 10M) was added into ice-cold iodobenzene (0.5 mL, 5 mmol) followed by 2-3 drops of 30%  $\text{H}_2\text{O}_2$ . Then the reaction mixture was allowed to stir for 2 hrs at 0 °C. The resulting orange solution gradually formed a yellow precipitate of solid product. The yellow precipitate was collected by filtration and  $\text{CH}_2\text{Cl}_2$  was slowly added to precipitate until completely dissolved. Dried the product using  $\text{MgSO}_4$ . The solution was then filtered into a 50 mL flask and stored in freezer to obtained pale yellow crystals. Yield, 1.23 g (99%).

#### Reaction of iodobenzene dichloride and pyridine for generation of crystalline **2**

Dichloroiodobenzene ( $\text{PhCl}_2$ ) (20 mg, 0.08 mmol) was dissolved in minimum amount of pyridine and stored in freezer to obtained yellow crystals.

#### Reaction of iodobenzene dichloride and pyridine for NMR analysis of **2**

Iodobenzene dichloride (20 mg, 0.0728 mmol) was dissolved in  $\text{CDCl}_3$  (0.6 mL) and rapidly stirred to give a pale-yellow solution. To this, pyridine (5.75 mg, 0.0728 mmol) was added in one portion and the reaction was left to stir. At t = 15 m, the reaction mixture was transferred to an NMR tube and taken for analysis.

#### Reaction of iodobenzene dichloride and 2,6-dimethylpyridine (Iutidine)

Iodobenzene dichloride (22 mg, 0.0808 mmol) was dissolved in  $\text{CDCl}_3$  (0.6 mL) and rapidly stirred to give a pale-yellow solution. To this, 2,6-dimethylpyridine (9 mg, 0.0808 mmol) was added in one portion and the reaction was left to stir. At t = 15 m, the reaction mixture was transferred to an NMR tube and taken for analysis.

#### Reaction of iodobenzene dichloride and 4-dimethylaminopyridine

Iodobenzene dichloride (200 mg, 0.728 mmol) was dissolved in  $\text{CHCl}_3$  (6 mL) in a reaction flask. 4-Dimethylaminopyridine (178 mg, 1.46 mmol) dissolved in  $\text{CHCl}_3$  (0.5 mL) was added to the flask. The mixture was stirred for 15 minutes. Subsequently, hexane was added to reaction mixture and a white solid precipitated. The precipitate was removed via centrifugation and identified as identified as 4-dimethylaminopyridine.HCl by  $^1\text{H}$  NMR via comparison with a genuine sample. The supernatant was collected, and volatiles were removed in vacuo to give a colourless liquid. The liquid was dissolved in  $\text{CHCl}_3$  (1 mL), and triflic acid (64  $\mu\text{L}$ , 0.728 mmol) was added dropwise with stirring. Diethyl ether (5 mL) was added to yield a white precipitate which was collected via centrifugation ( $m/z$  = 157.13). The solid was dissolved in  $\text{H}_2\text{O}$  (1 mL) and basified with 1M NaOH (approx. 1 mL) until pH 14. The aqueous solution was extracted with  $\text{CH}_2\text{Cl}_2$  (3 x 5 mL). The organic layers were combined and washed with  $\text{H}_2\text{O}$  (3 x 10 mL) and subsequently dried over  $\text{MgSO}_4$  and filtered. Volatiles were removed in vacuo to give **3** as a colourless liquid (70 mg, 61%).

$^1\text{H}$  NMR, ppm ( $\text{CDCl}_3$ , 400 MHz):  $\delta$  8.32 (1H, s), 8.22-8.20 (1H, d), 6.75-6.74 (1H, d), 2.99 (6H, s).

$^{13}\text{C}$  NMR, ppm ( $\text{CDCl}_3$ ):  $\delta$  155.50, 150.24, 147.68, 121.66, 112.82, 42.32.

## 2. Data collection and details of structure refinement

X-ray data were collected using either a Rigaku XtaLAB Synergy, Dualflex, Pilatus 300K diffractometer or a Rigaku SuperNova. Using Olex2<sup>1</sup>, the structures were solved with the SHELXT<sup>2</sup> structure solution program using Intrinsic Phasing and refined with the SHELXL<sup>3</sup> refinement package using Least Squares minimisation. Crystal data and information concerning data collection is shown in the following table. CCDC Deposition Numbers 2071297-2071290 may be used to access the Crystallographic Information Files (.cif) from the Cambridge Crystallographic Data Centre.

Table S1. Crystal data and structure refinement for PhICl<sub>2</sub>, **2** and **3**

Identification code	PhICl <sub>2</sub>	<b>2</b>	<b>3</b>
Empirical formula	C <sub>6</sub> H <sub>5</sub> Cl <sub>2</sub> I	C <sub>11</sub> H <sub>10</sub> Cl <sub>2</sub> IN	C <sub>8</sub> H <sub>10</sub> ClF <sub>3</sub> N <sub>2</sub> O <sub>3</sub> S
Formula weight	274.90	354.00	306.69
Temperature/K	100(2)	100(2)	150(2)
Crystal system	monoclinic	monoclinic	monoclinic
Space group	P2 <sub>1</sub> /n	P2 <sub>1</sub> /n	P2 <sub>1</sub> /n
a/Å	12.0910(2)	8.9394(3)	7.7784(2)
b/Å	5.35790(10)	15.5397(4)	9.3743(2)
c/Å	12.42400(10)	9.5747(3)	16.8499(5)
α/°	90	90	90
β/°	101.8700(10)	107.339(4)	95.923(3)
γ/°	90	90	90
Volume/Å <sup>3</sup>	787.65(2)	1269.63(7)	1222.09(6)
Z	4	4	4
ρ <sub>calc</sub> g/cm <sup>3</sup>	2.318	1.852	1.667
μ/mm <sup>-1</sup>	2.448	2.911	4.807
F(000)	512.0	680.0	624.0
Crystal size/mm <sup>3</sup>	0.15 × 0.12 × 0.04	0.12 × 0.09 × 0.04	0.18 × 0.15 × 0.06
Radiation	Ag Kα (λ = 0.56087)	Mo Kα (λ = 0.71073)	Cu Kα (λ = 1.54184)
2θ range for data collection/°	5.288 to 95.114	5.17 to 50.244	10.556 to 142.59
Index ranges	-31 ≤ h ≤ 31, -14 ≤ k ≤ 14, -32 ≤ l ≤ 32	-10 ≤ h ≤ 10, -18 ≤ k ≤ 18, -11 ≤ l ≤ 11	-9 ≤ h ≤ 9, -11 ≤ k ≤ 10, -19 ≤ l ≤ 20
Reflections collected	112670	12645	11583
Independent reflections	15027 [R <sub>int</sub> = 0.0387, R <sub>sigma</sub> = 0.0180]	2263 [R <sub>int</sub> = 0.0512, R <sub>sigma</sub> = 0.0303]	2360 [R <sub>int</sub> = 0.0324, R <sub>sigma</sub> = 0.0253]
Data/restraints/parameters	15027/0/82	2263/0/136	2360/0/169
Goodness-of-fit on F <sup>2</sup>	1.051	1.055	1.063
Final R indexes [I>=2σ (I)]	R <sub>1</sub> = 0.0162, wR <sub>2</sub> = 0.0394	R <sub>1</sub> = 0.0338, wR <sub>2</sub> = 0.0773	R <sub>1</sub> = 0.0788, wR <sub>2</sub> = 0.2045
Final R indexes [all data]	R <sub>1</sub> = 0.0208, wR <sub>2</sub> = 0.0403	R <sub>1</sub> = 0.0358, wR <sub>2</sub> = 0.0786	R <sub>1</sub> = 0.0857, wR <sub>2</sub> = 0.2133
Largest diff. peak/hole / e Å <sup>-3</sup>	1.99/-0.90	2.87/-1.86	1.87/-0.53

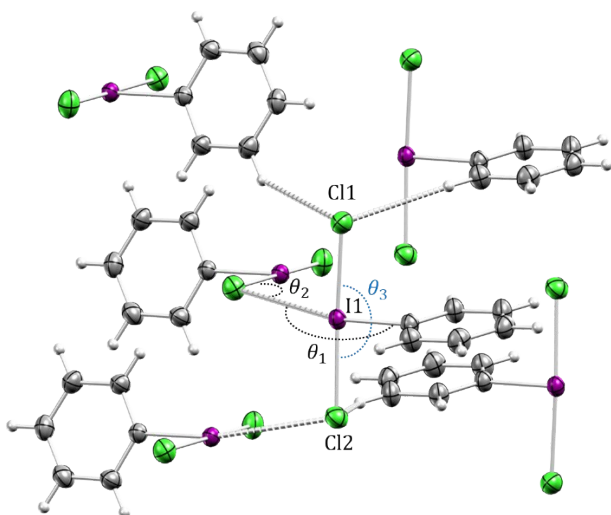


Figure S1: Crystal packing in  $\text{PhICl}_2$ . Angles:  $\theta_1(\text{C}-\text{I} \star \star \star \text{Cl}) = 166.38^\circ$ ,  $\theta_2(\text{Cl}-\text{I} \star \star \star \text{Cl}) = 100.24^\circ$ ,  $\theta_3(\text{Cl}-\text{I}-\text{Cl}) = 176.70^\circ$ ; bond distances  $d(\text{I}-\text{Cl}1) = 2.48319(12)$  Å and  $d(\text{I}-\text{Cl}2) = 2.505926(11)$  Å. The slightly asymmetrical I-Cl distances can be attributed to different intermolecular interactions. The Cl2 atom interacts with the iodine I1 *via* a type II  $\beta$  halogen bonding ( $\psi = 0.33$ )<sup>4</sup> while Cl1 atom undergoes exclusively hydrogen bonding interactions with two aryl C-Hs.

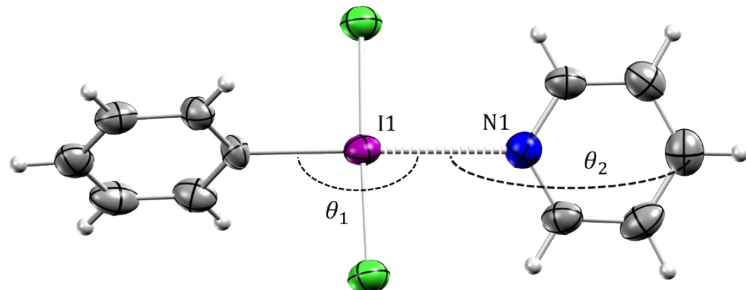


Figure S2: Crystal structure of the  $\text{PhICl}_2 \star \text{Py}$  aggregate **2**. Selected angles ( $\theta_1(\text{C}-\text{I} \star \star \star \text{Cl}) = 177.97^\circ$ ,  $\theta_2(\text{Cl}-\text{I} \star \star \star \text{Cl}) = 175.38^\circ$ ) show a type II  $\beta$  halogen bonding ( $\psi = 0.98$ )<sup>4</sup> with an intermolecular short contact distance of  $d(\text{N1} \star \star \star \text{I1}) = 2.750$  Å.

### 3. Experimental electron density study

#### 3.1. Multipole refinement of PhICl<sub>2</sub>

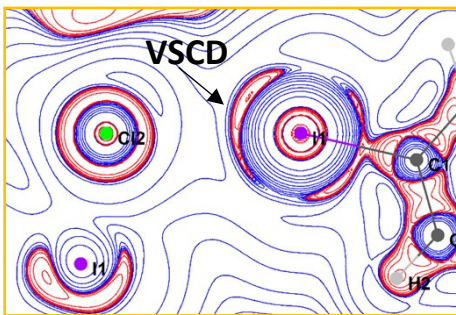
The multipolar refinement was carried out on  $F^2$  according to the Hansen & Coppens formalism for aspherical atomic density expansion as implemented in *MoProSuite*.<sup>5,6</sup> Multipole coefficients up to hexadecapoles were refined for non-H atoms. H-atoms were constrained to C-H bond distances of 1.083 Å based on neutron diffraction data reported by Allen and Bruno.<sup>7</sup> Refinement results have been compiled in Table 2. Electron density maps were obtained using *MoProViewer*.<sup>8</sup>

Table S2: Refinement results.

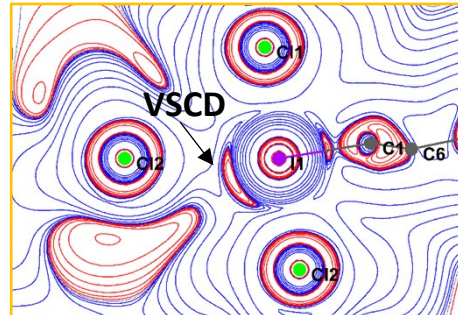
Refinement	IAM	MM
Resolution	0.38 – 10 Å	0.38 – 6.079 Å
R <sub>1</sub> [ $ I  \geq 2\sigma(I)$ ]	0.0162	0.01296 (RF factor)
wR <sub>2</sub> [ $ I  \geq 2\sigma(I)$ ]	0.0394	0.01360 (wR2F factor)
R <sub>1</sub> [all data]	0.0208	0.01910 (RI factor)
wR <sub>2</sub> [all data]	0.0403	0.02.668 (wR2I factor)
Nvar/Nref	-	301/11758
Largest diff. peak/hole / e Å <sup>-3</sup>	1.99/-0.90	-
Goodness-of-fit on $F^2$	1.051	1.028
Weighting scheme	0.0177 0.0497	0.52372 (MoPro gof1)

#### 3.2. Topological analysis

a)



b)



c)

d)

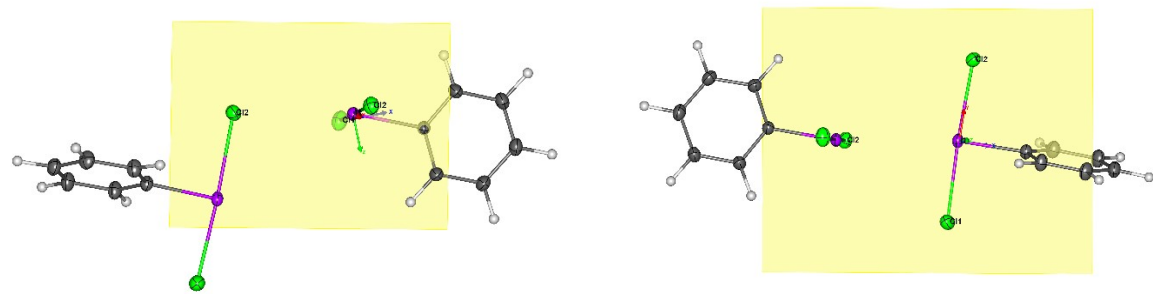


Figure S3: Logarithmic Laplacian maps of the intermolecular halogen bonding  $I1 \rightarrow Cl2$  along the ZX plane **a)** and XY plane **b)** and **d)**. Red denotes charge depletion (VSCD) and blue denotes charge concentration (VSAC).

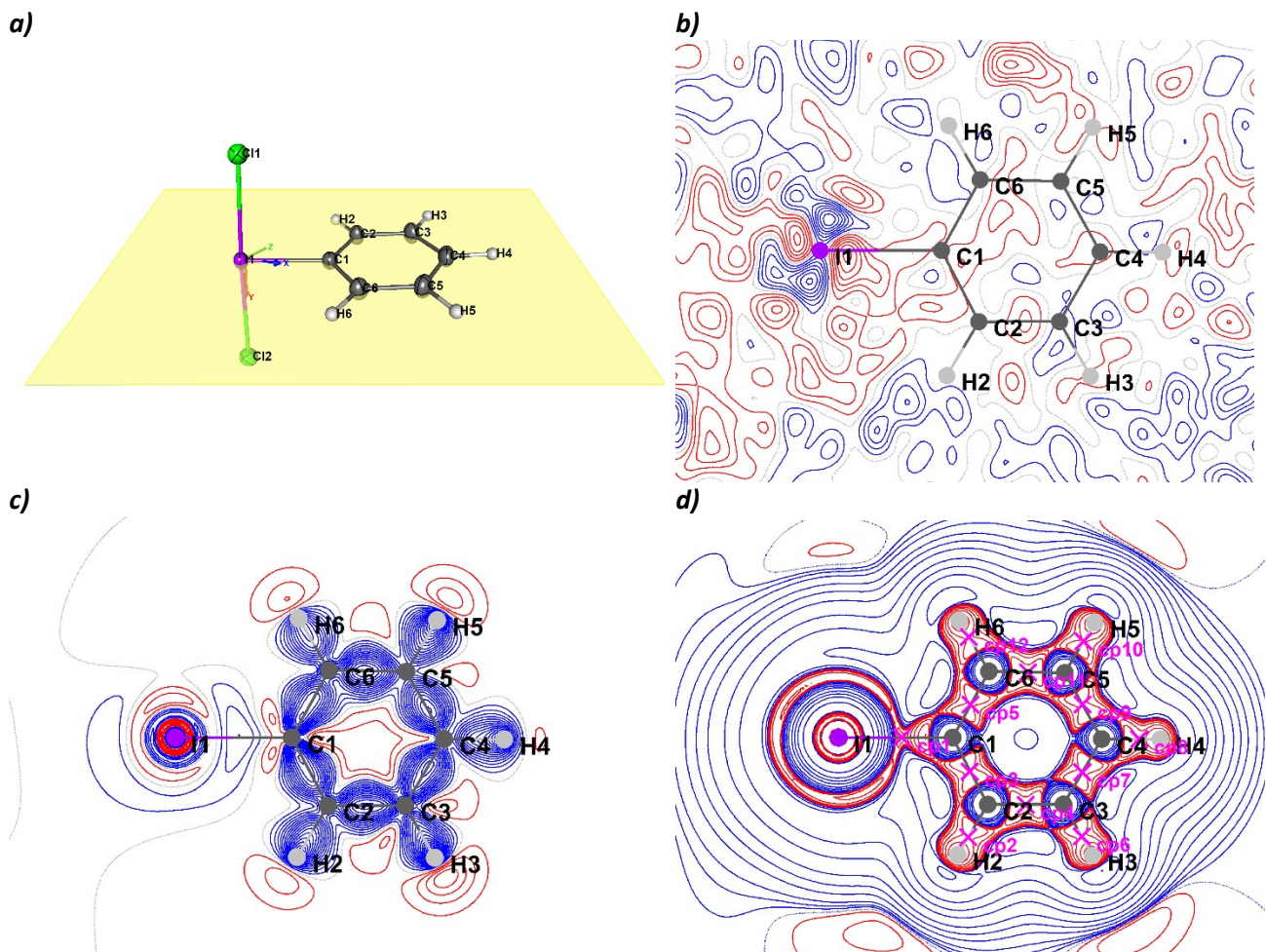
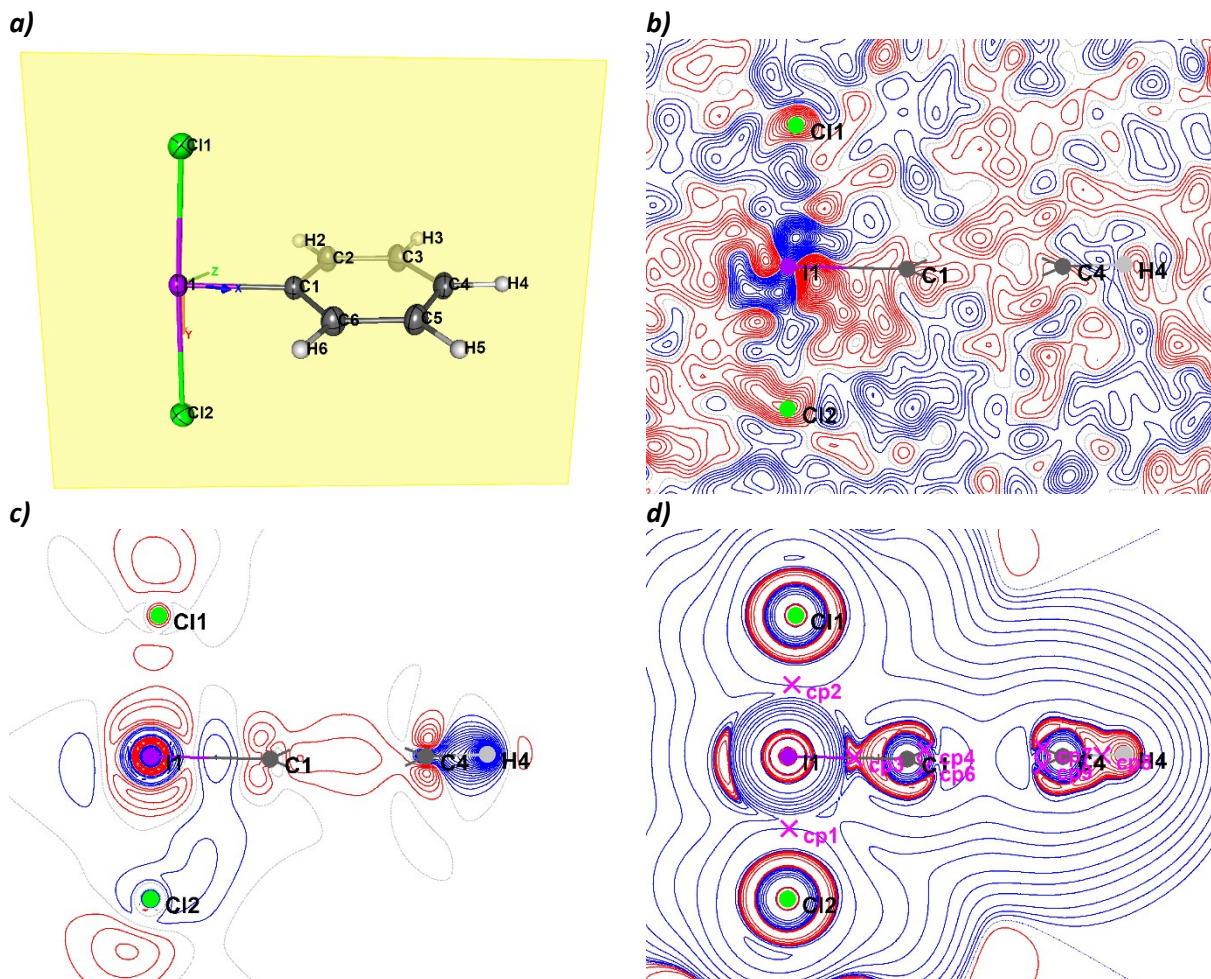
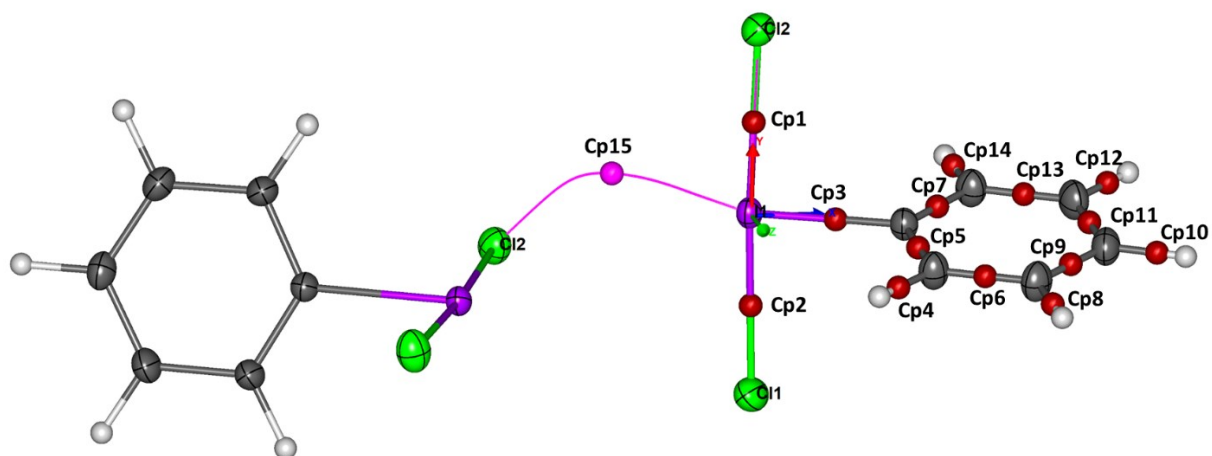


Figure S4: Experimental two-dimensional electron density maps of **1** at a resolution range of  $0.38 < d (\text{\AA}) > 6.079$ . **a)** shows the ZX plane used for 2D maps, **b)** corresponds to the residual density ( $0.10 \text{ e \AA}^{-3}$ ,  $0.08 < \sin\theta/\lambda < 0.80$ ), **c)** full deformation of the static electron density (contour  $0.05 \text{ e \AA}^{-3}$ ). Positive density is shown in blue and negative in red; grey dotted lines represent zero density. The Laplacian map of iodobenzene dichloride **d)** was drawn on a logarithmic scale. Red denotes charge depletion (VSCD) and blue denotes charge concentration (VSAC).



**Figure S5:** Experimental two-dimensional electron density maps of **1** at a resolution range of  $0.38 < d (\text{\AA}) > 6.079$ . **a)** shows the XY plane used for 2D maps, **b)** corresponds to the residual density ( $0.10 \text{ e } \text{\AA}^{-1}, 0.08 < \sin\theta/\lambda < 0.80$ ), **c)** full deformation of the static electron density (contour  $0.05 \text{ e } \text{\AA}^{-1}$ ). Positive density is shown in blue and negative in red; grey dotted lines represent zero density. The Laplacian map of iodobenzene dichloride **d)** was drawn on a logarithmic scale. Red denotes charge depletion (VSCD) and blue denotes charge concentration (VSCC).



**Figure S6:** Non-covalent ● and covalent ● critical points of **1** illustrated with MoProViewer.



$d_{ij}$  is the bond path,  $d_1$  and  $d_2$  its components,  $\rho$  the electron density and  $\Delta^2$  the Laplacian in the intermolecular bcp.

#### 4. NMR Investigations

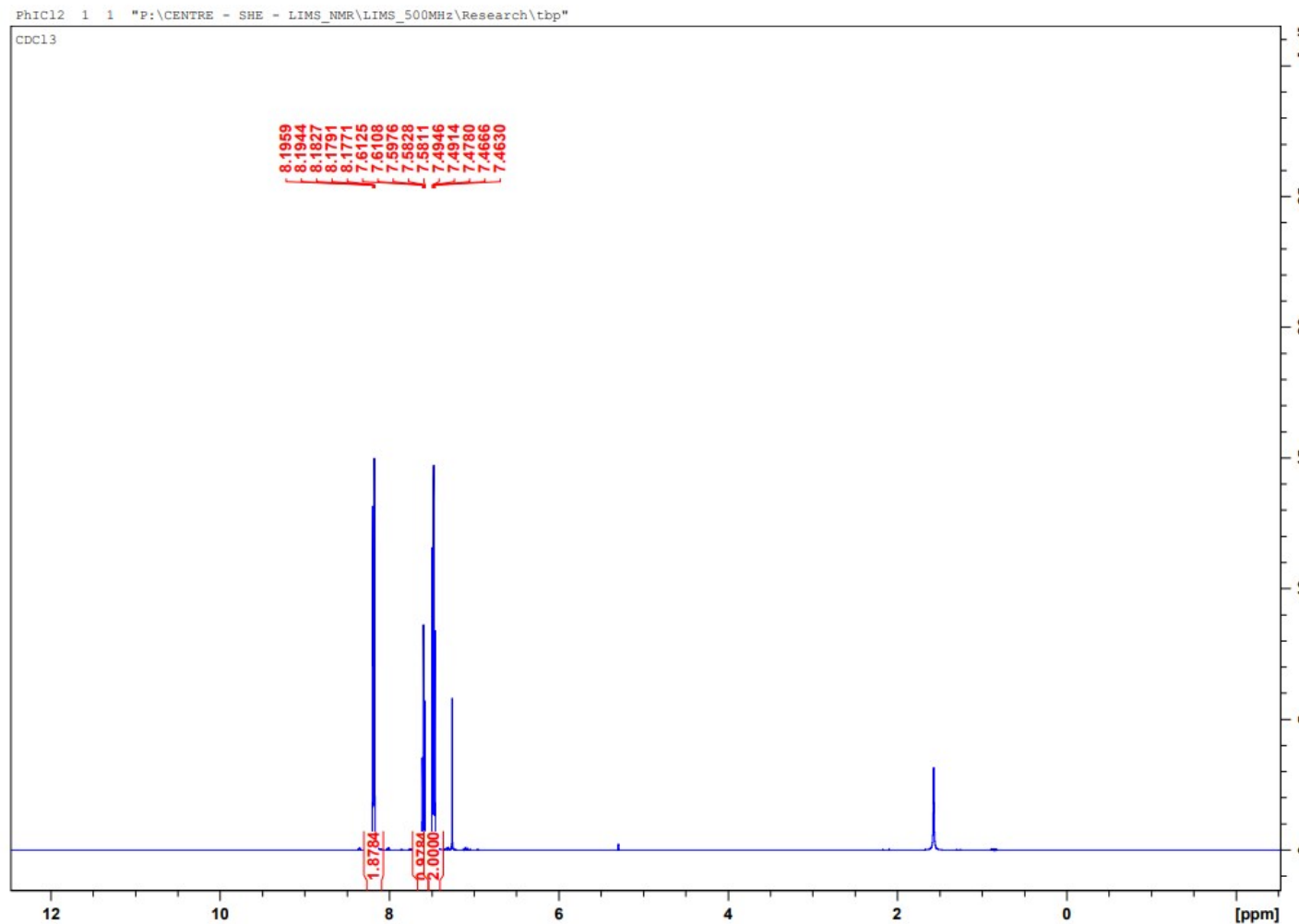
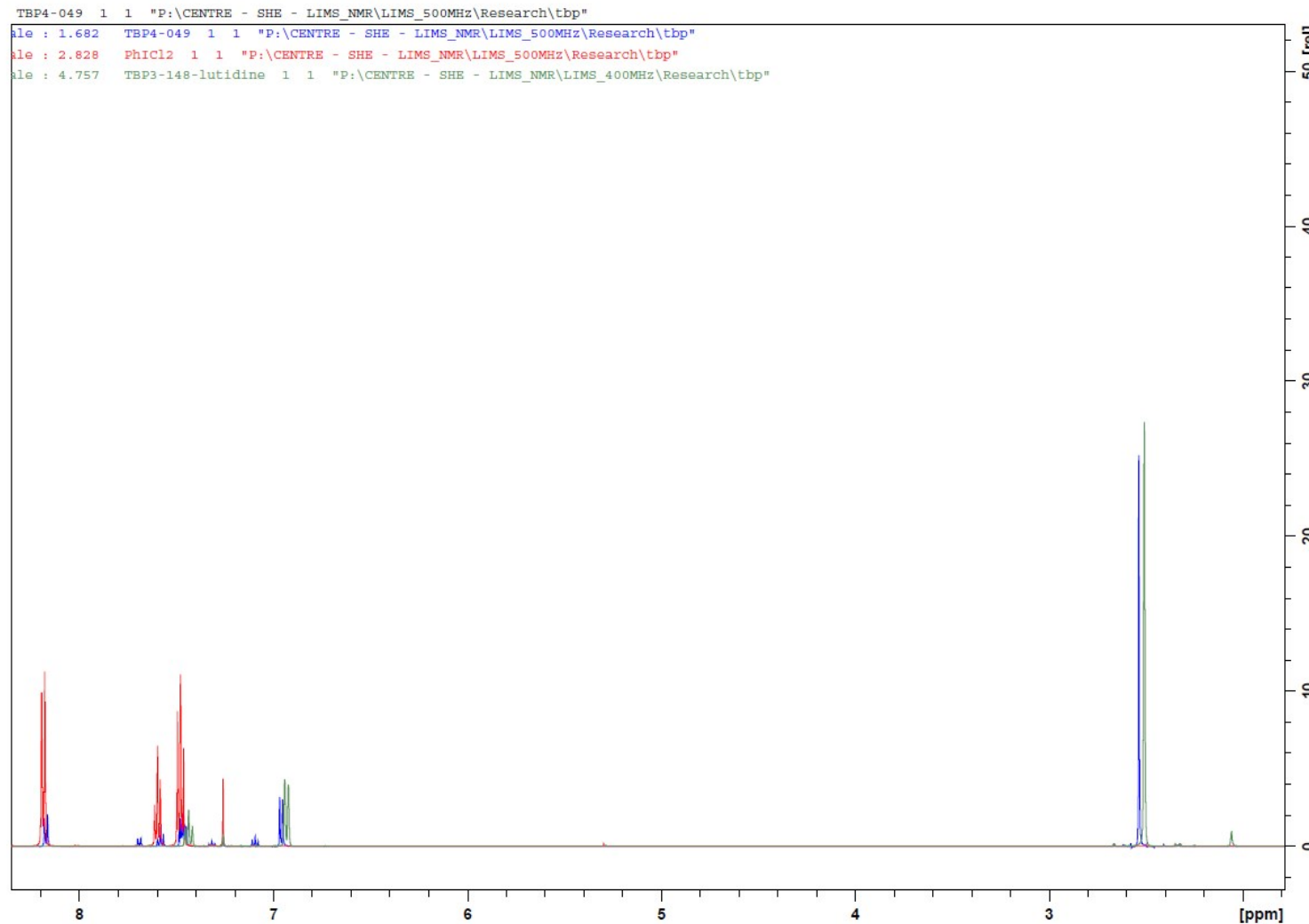
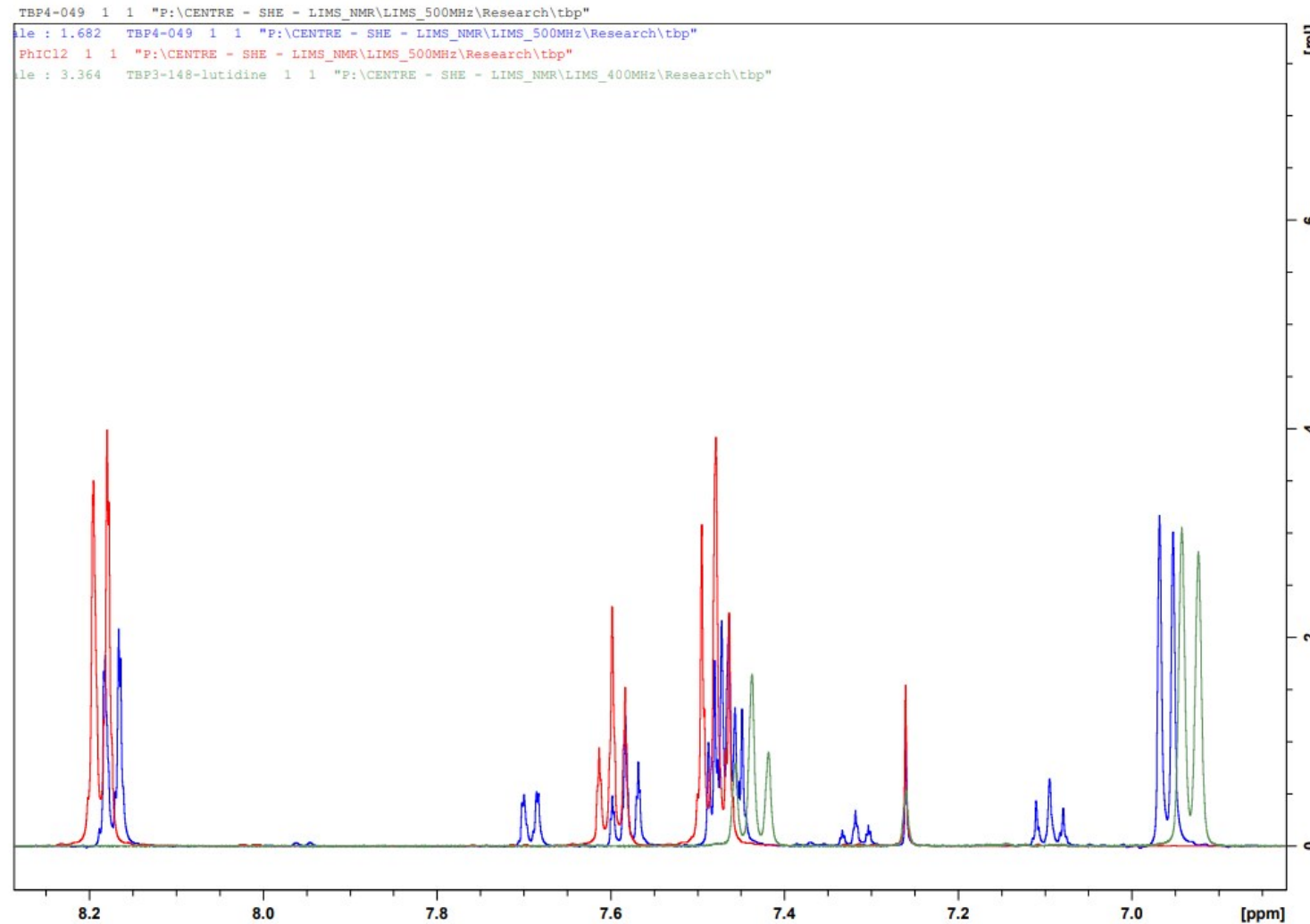


Figure S7: Iodobenzene dichloride in CDCl<sub>3</sub>.



**Figure S2:** Reaction mixture of PhICl<sub>2</sub> and 2,6-dimethylpyridine (blue) overlayed with PhICl<sub>2</sub> (red) and 2,6-dimethylpyridine (green) in CDCl<sub>3</sub>.



**Figure S3:** Downfield region of reaction mixture of PhICl<sub>2</sub> and 2,6-dimethylpyridine (blue) overlayed with PhICl<sub>2</sub> (red) and 2,6-dimethylpyridine (green).

**Note:** Free iodobenzene is present owing to gradual decomposition of PhICl<sub>2</sub>.

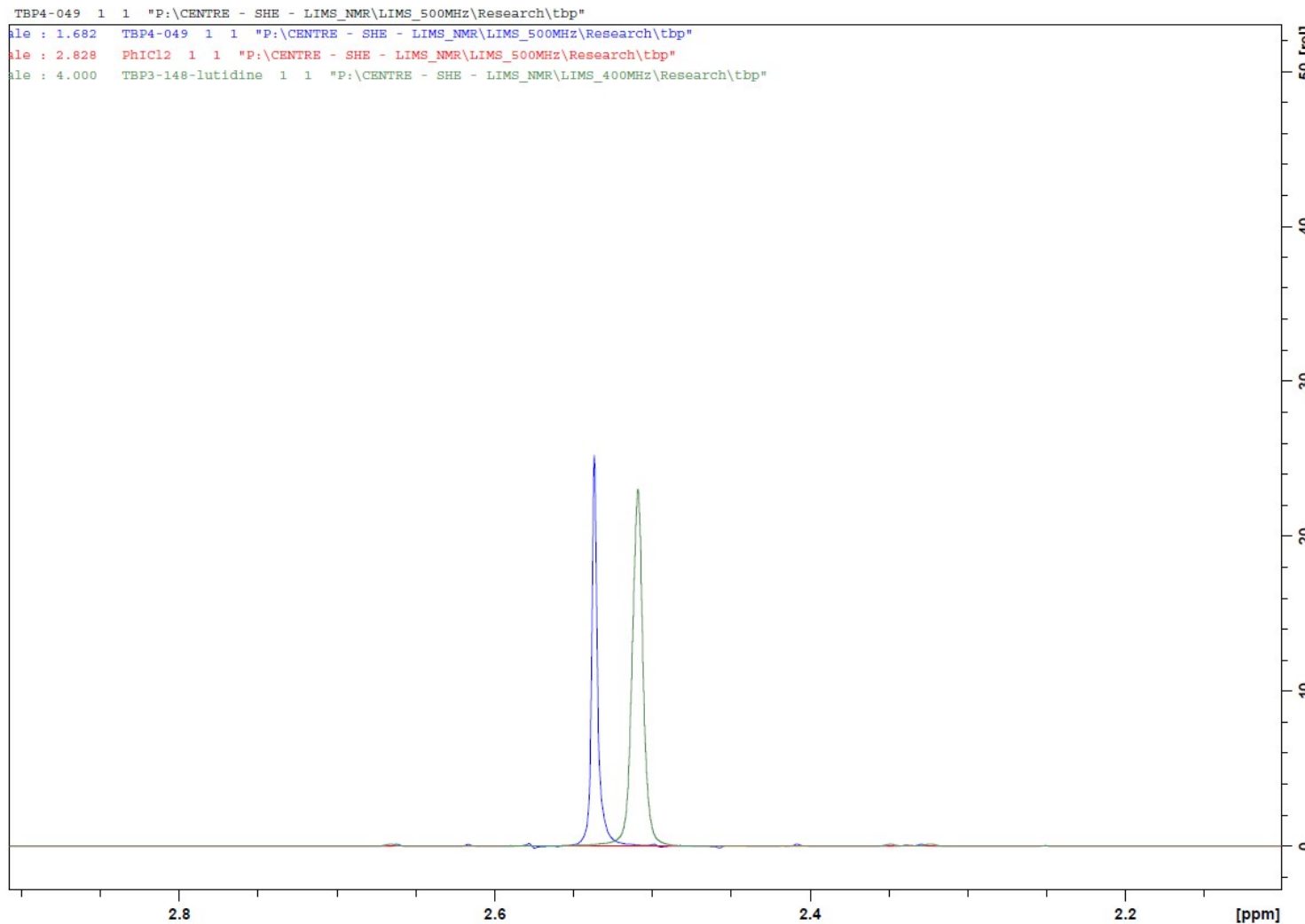


**Figure S4:** Upfield region of reaction mixture of PhICl<sub>2</sub> and 2,6-dimethylpyridine (blue) overlaid with PhICl<sub>2</sub> (red) and 2,6-dimethylpyridine (green).

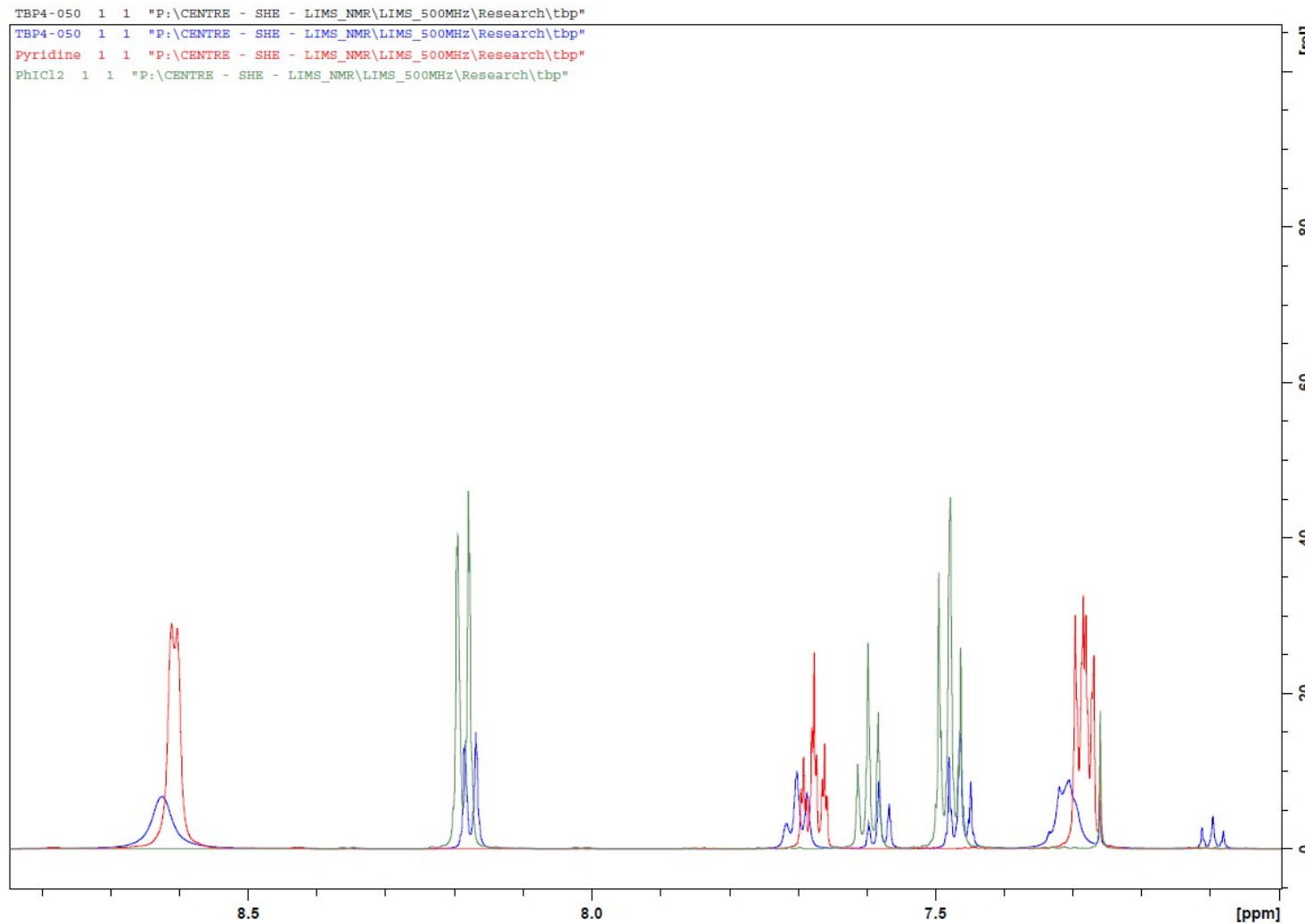


**Figure S5:** Reaction mixture of PhICl<sub>2</sub> and pyridine (blue) overlayed with PhICl<sub>2</sub> (green) and pyridine (red).

**Note:** Free iodobenzene is present owing to gradual decomposition of PhICl<sub>2</sub>

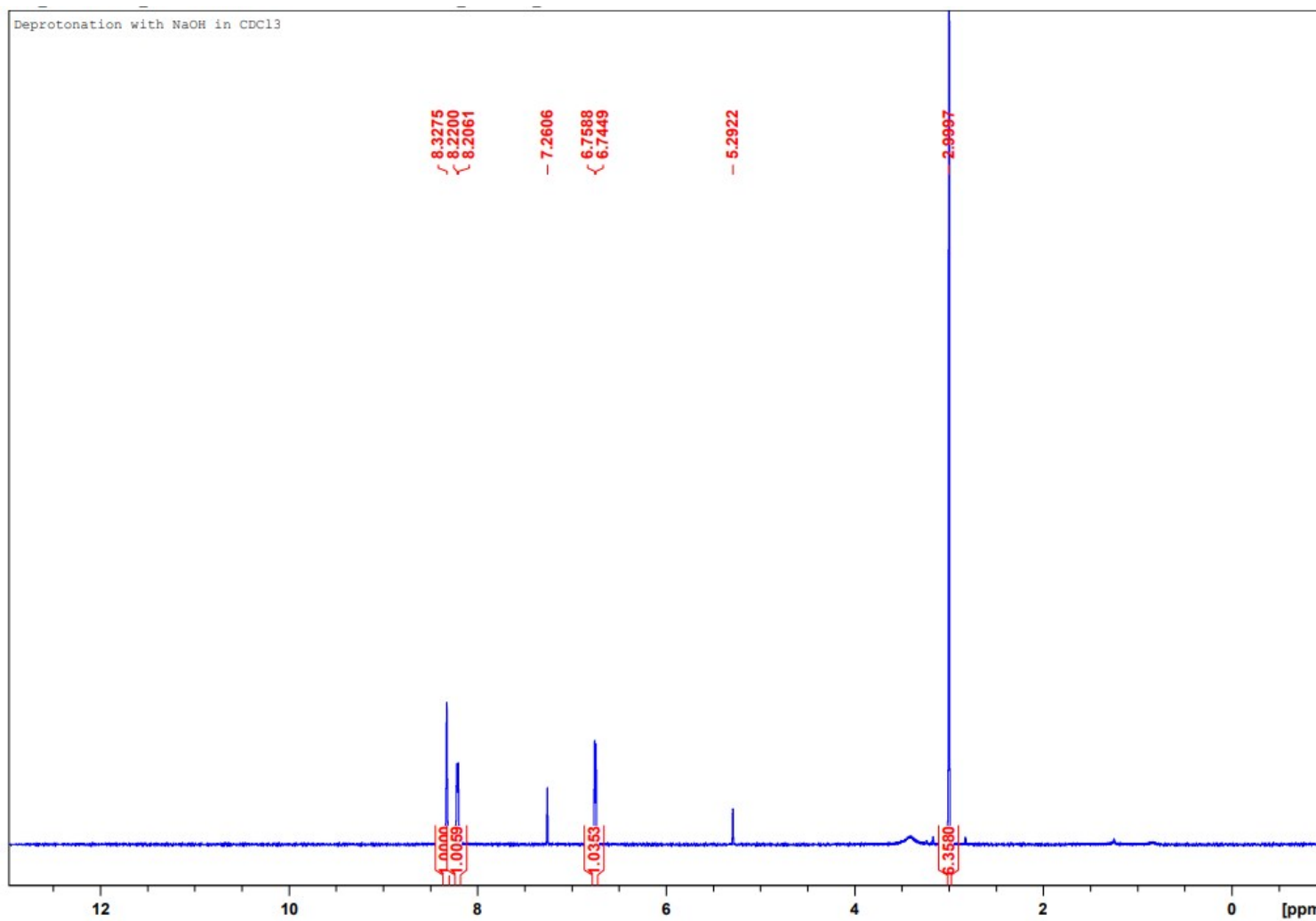


**Figure S6:** <sup>1</sup>H spectrum of 3-chloro-4-dimethylaminopyridine in CDCl<sub>3</sub>.

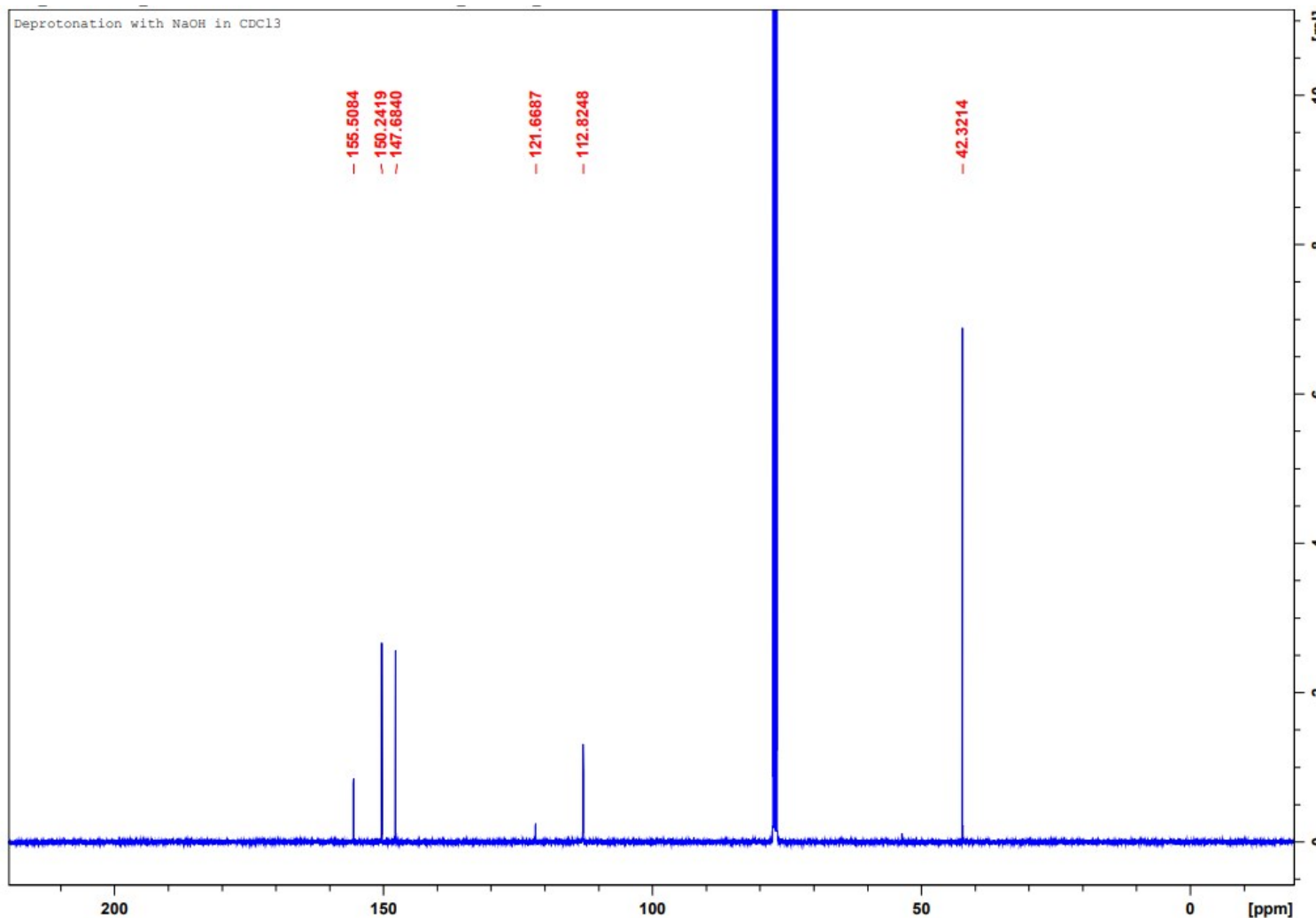


**Figure S7:**  $^{13}\text{C}$  spectrum of 3-chloro-4-dimethylaminopyridine in  $\text{CDCl}_3$

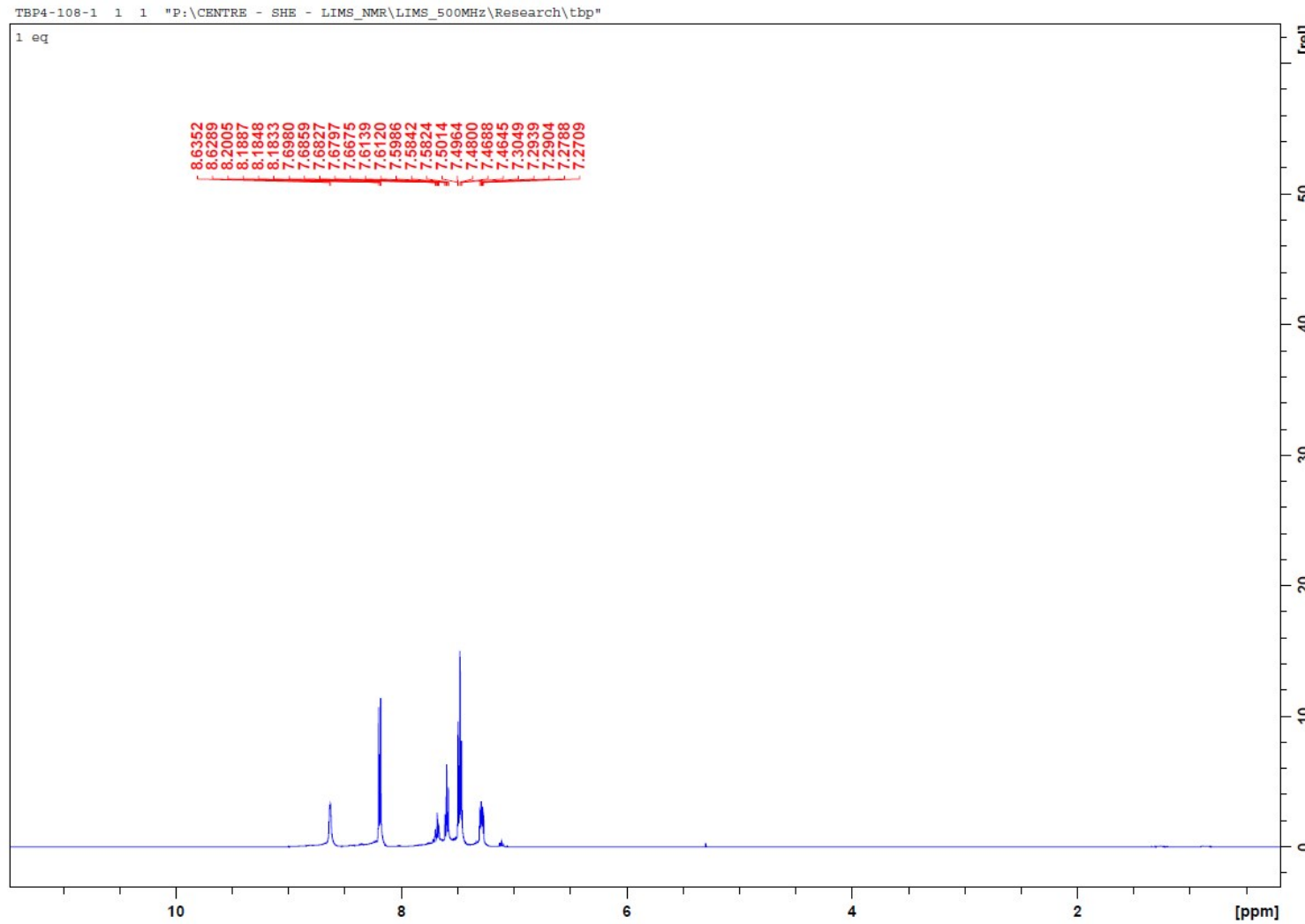


**Figure S8:**  $^1\text{H}$  NMR spectrum of 1 equivalent of  $\text{PhICl}_2$  and 1 equivalent of pyridine in  $\text{CDCl}_3$ .

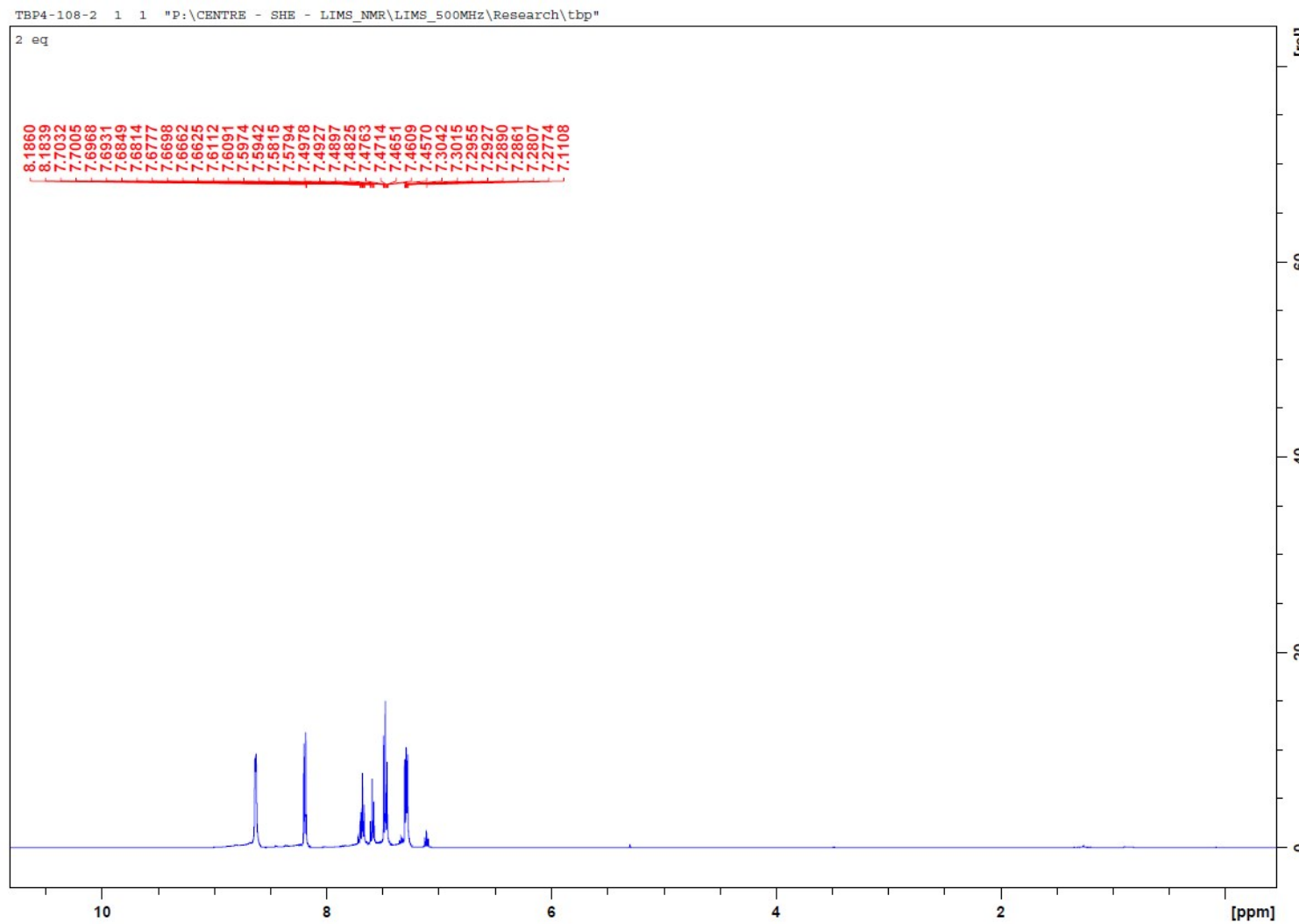


**Figure S9:**  $^1\text{H}$  NMR spectrum of 1 equivalent of  $\text{PhICl}_2$  and 2 equivalents of pyridine in  $\text{CDCl}_3$ .

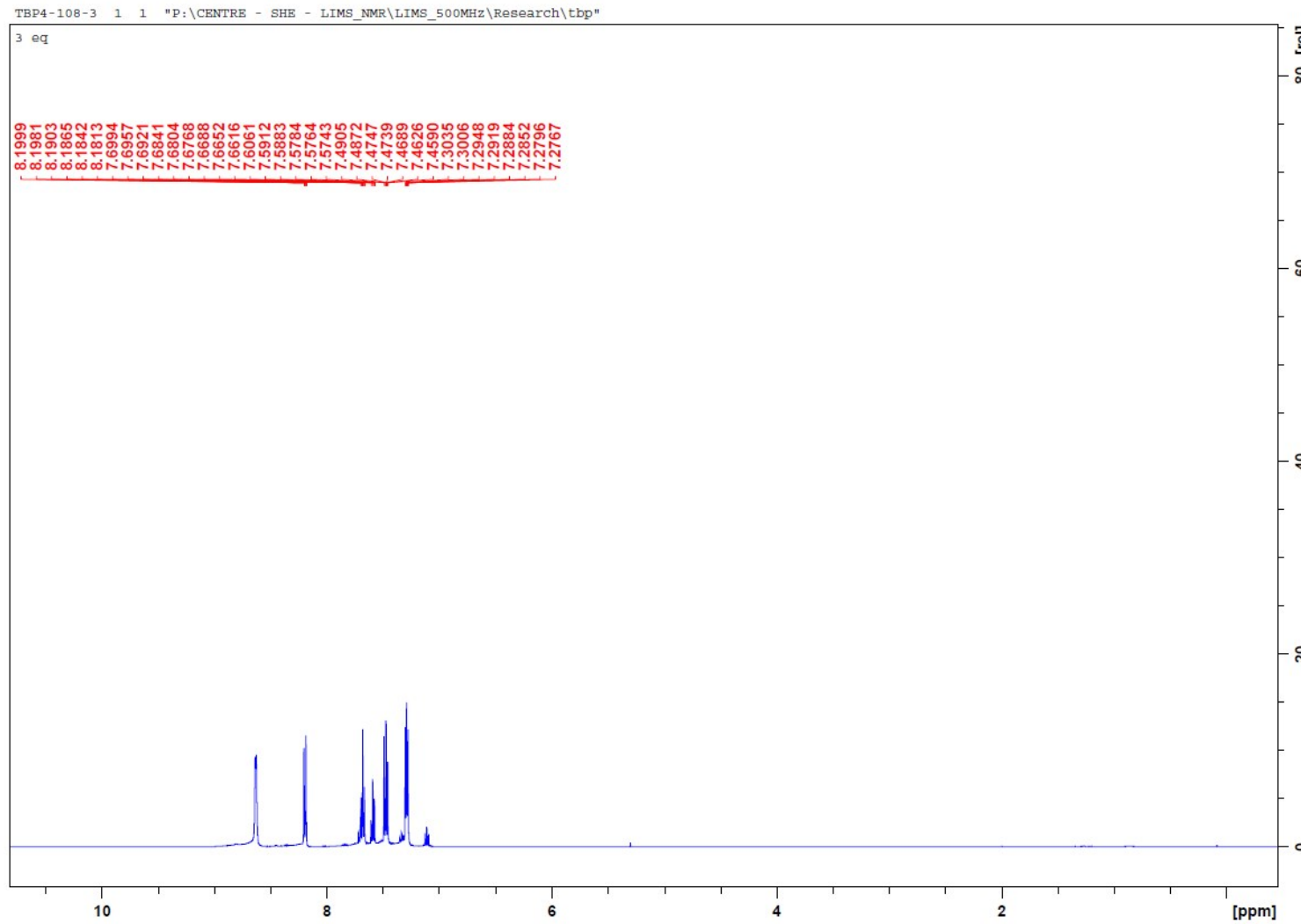


**Figure S10:** <sup>1</sup>H NMR spectrum of 1 equivalent of PhICl<sub>2</sub> and 3 equivalents of pyridine in CDCl<sub>3</sub>.

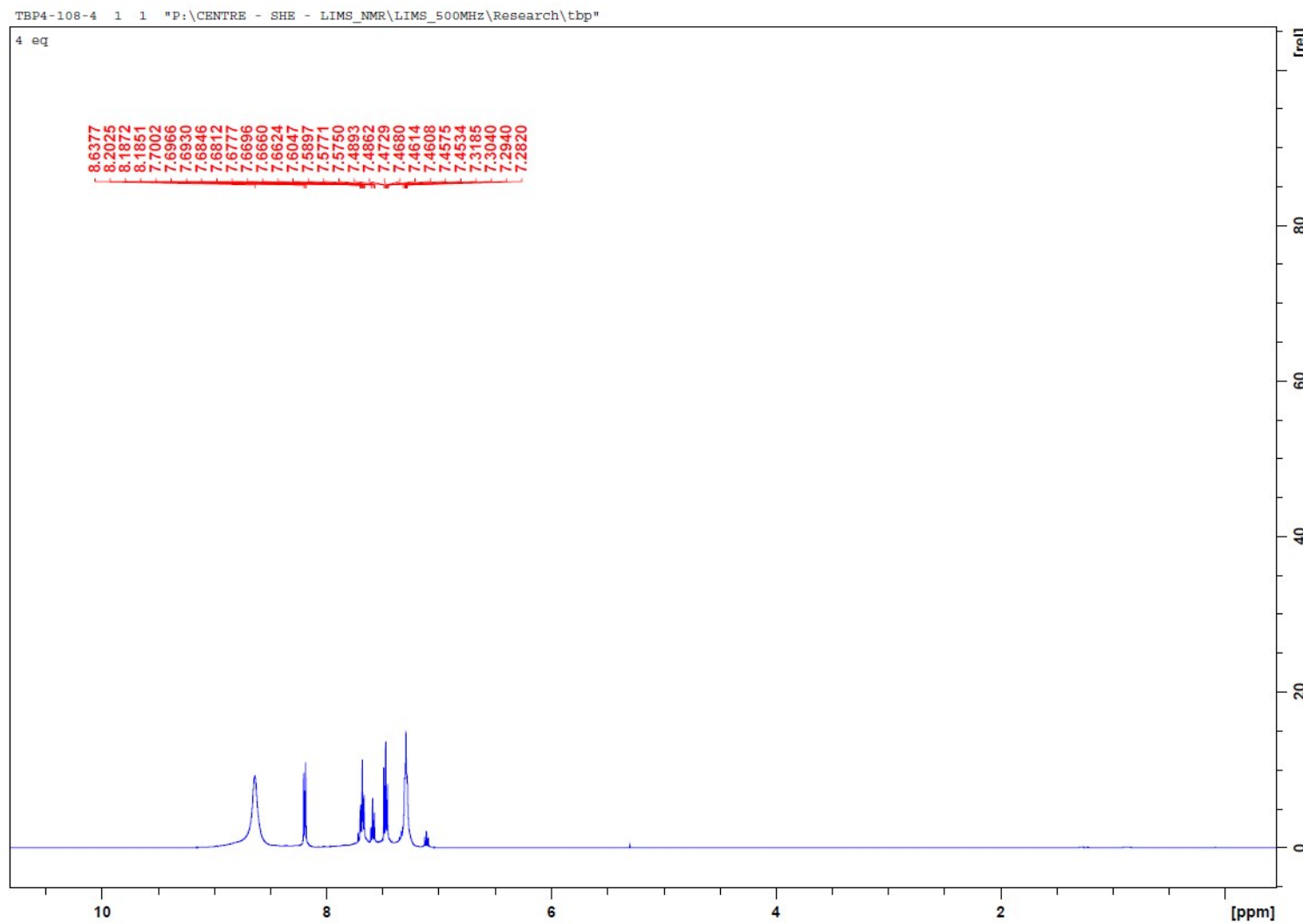


**Figure S11:**  $^1\text{H}$  NMR spectrum of 1 equivalent of  $\text{PhICl}_2$  and 4 equivalents of pyridine in  $\text{CDCl}_3$ .

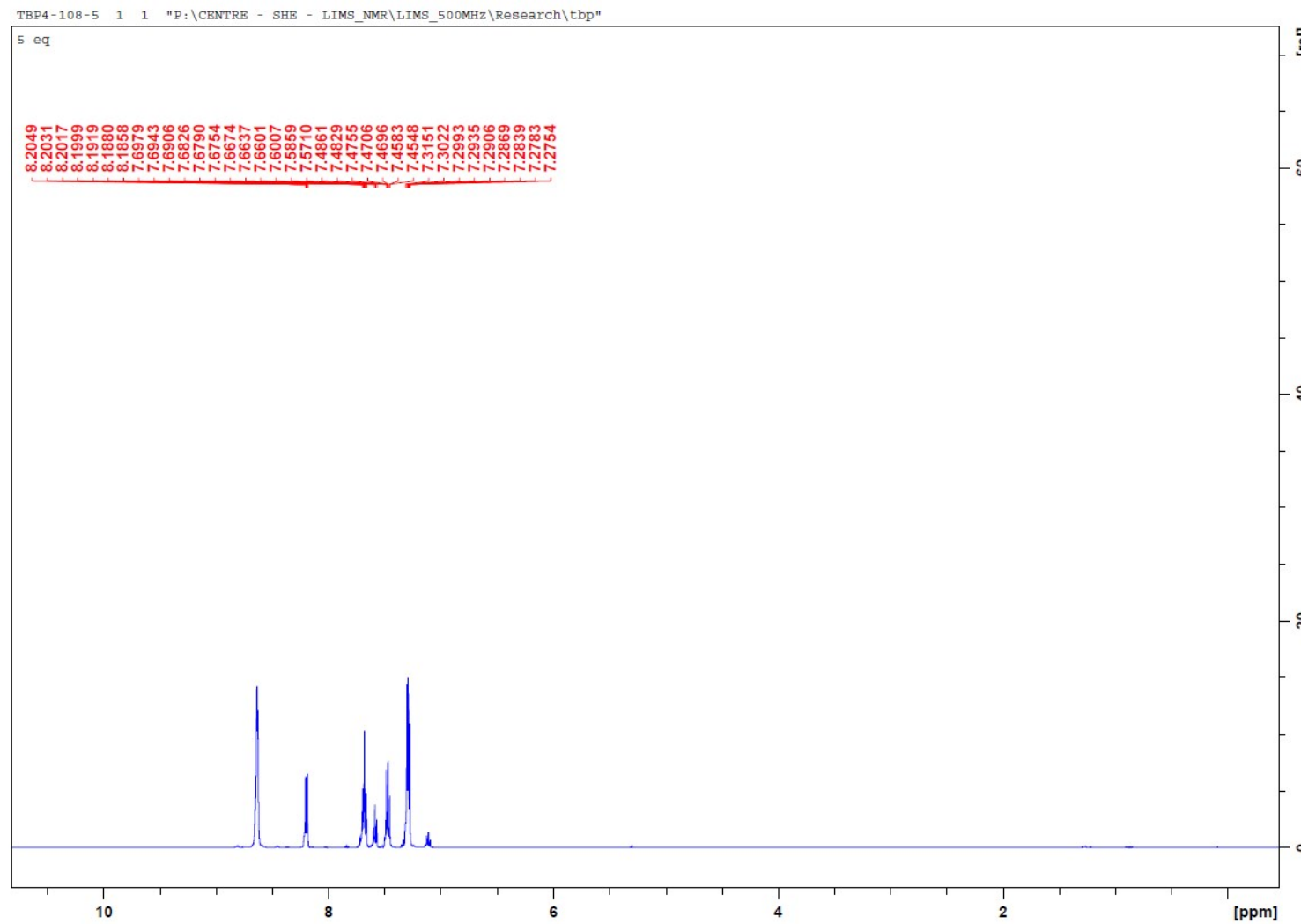


**Figure S12:**  $^1\text{H}$  NMR spectrum of 1 equivalent of  $\text{PhICl}_2$  and 5 equivalents of pyridine in  $\text{CDCl}_3$ .

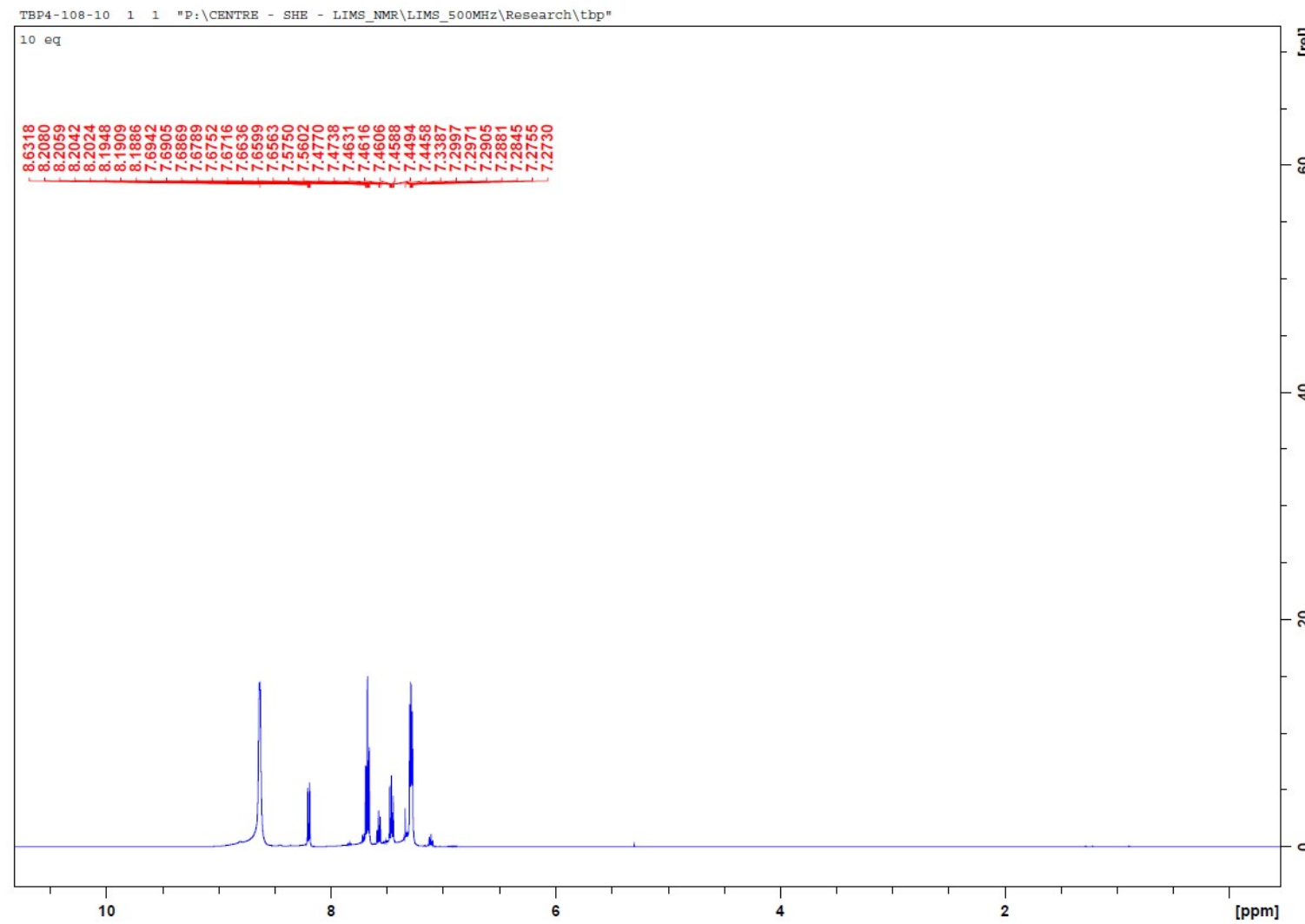


**Figure S13:**  $^1\text{H}$  NMR spectrum of 1 equivalent of  $\text{PhI(Cl)}_2$  and 10 equivalents of pyridine in  $\text{CDCl}_3$ .

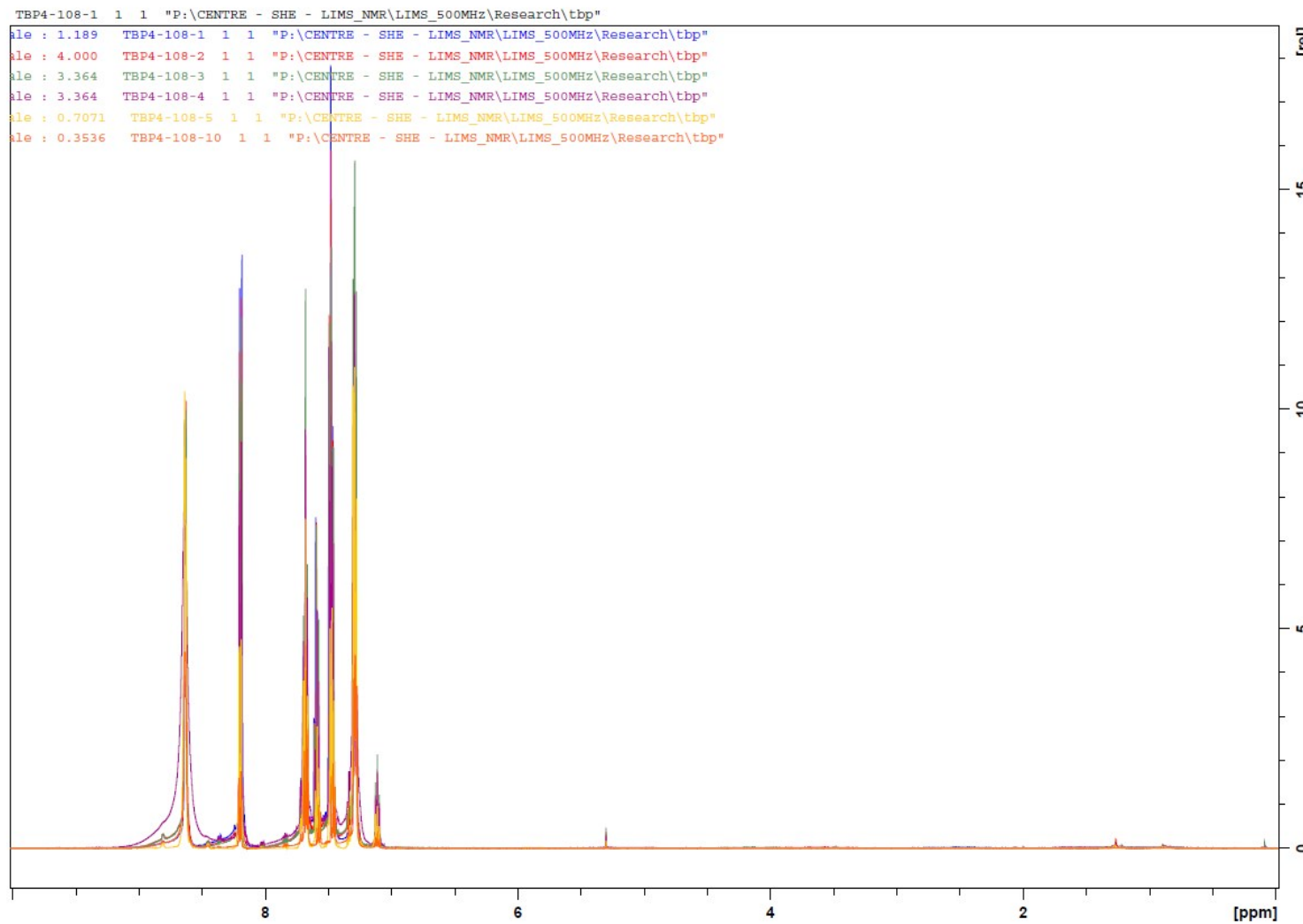


**Figure S14:**  $^1\text{H}$  NMR spectrum overlay of  $\text{PhICl}_2$  and 1-5, 10 equivalents of pyridine in  $\text{CDCl}_3$ .

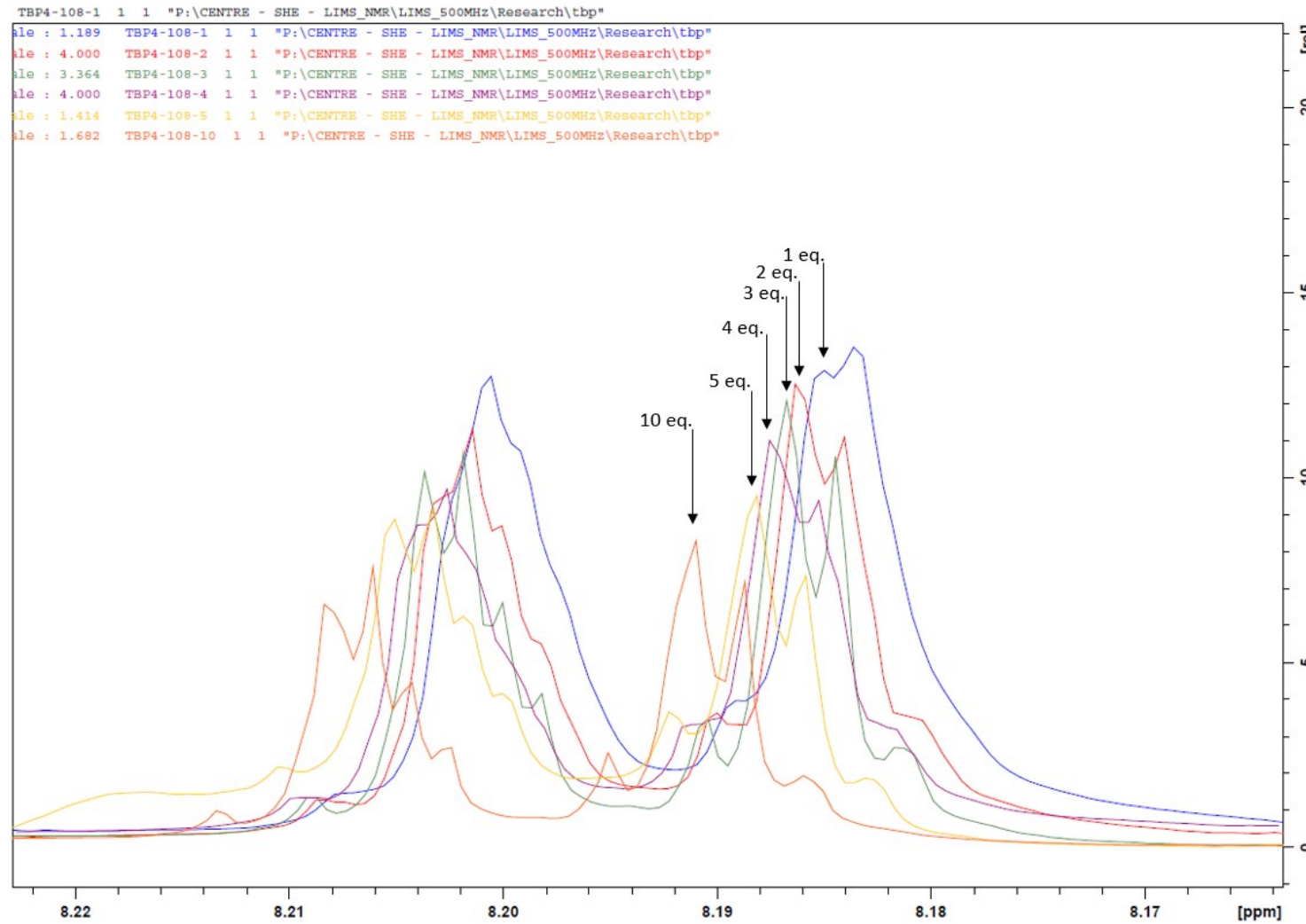


**Figure S15:**  $^1\text{H}$  NMR spectrum overlay (most downfield signal) of  $\text{PhICl}_2$  and 1-5, 10 equivalents of pyridine in  $\text{CDCl}_3$ .

## 5. Computational details

All calculations were performed using Gaussian 16 revision A.03 unless noted.<sup>18</sup> Geometry optimizations were performed with the B3LYP density functional<sup>19, 20</sup> with Grimme's empirical D3 dispersion with Becke-Johnson (BJ) damping,<sup>21</sup> together with the def2-TZVPPD basis set, which includes an ECP for iodine.<sup>21, 22</sup> Harmonic vibrational frequencies were computed analytically at the same level of theory in order to characterise the stationary points as minima on the potential energy surface and determine thermochemical properties. Geometry optimization and harmonic frequency calculations inclusive of solvent effects using the polarizable continuum model (IEF-PCM) with Truhlar's SMD model<sup>23</sup> with parameters for acetonitrile.

All subsequent property and electronic structure calculations were carried out at the optimized geometries. Molecular orbital (MO), population analysis (CM5 charges<sup>24</sup>) and Natural Bond Orbital (NBO) analysis was carried out at the same B3LYP-D3(BJ)/def2-TZVPPD (SMD, acetonitrile) level of theory. NBO analysis was performed using NBO 6.0.<sup>25</sup>

For thermochemistry analysis, single point calculations were carried out at the  $\omega$ B97XD/def2-TZVPPD, B3LYP-D3(BJ)/def2-QZVPPD level of theory.<sup>23</sup> All calculations included SMD solvation with acetonitrile, while B3LYP-D3(BJ)/def2-QZVPPD calculations were also carried out with dichloromethane and pyridine solvation. Single-point DLPNO-CCSD(T)/def2-QZVPP calculations (inclusive of CPCM acetonitrile solvation) were computed using ORCA 4.2.1.<sup>26</sup> The single point energies were converted to free energies ( $\Delta G$ ) by adding the free energy correction calculated at the B3LYP-D3(BJ)/def2-TZVPPD (SMD, acetonitrile) level of theory in the harmonic frequency calculation. Thermochemistry analysis with quasi-harmonic analysis was carried out in GoodVibes 3.0.2.<sup>27</sup>

Table S6. Calculated  $\Delta G$  of reaction (kJ/mol) for addition of pyridine to PhICl<sub>2</sub> to form four-coordinate PhICl<sub>2</sub>pyr (compound **2**).

Method	Basis Set	Solvation	Geometry	$\Delta G$	$\Delta G(QH)^a$
B3LYP-D3(BJ)	Def2-TZVPPD	Gas phase	opt	-10.1	-14.0
B3LYP-D3(BJ)	Def2-TZVPPD	ACN	opt	+11.6	+9.3
$\omega$ B97XD	Def2-TZVPPD	ACN	opt	+17.1	+15.1
B3LYP-D3(BJ)	Def2-QZVPPD	ACN	b	+12.1	+9.3
B3LYP-D3(BJ)	Def2-QZVPPD	CH <sub>2</sub> Cl <sub>2</sub>	b	+10.8	+8.5
B3LYP-D3(BJ)	Def2-QZVPPD	pyridine	b	+10.5	+8.2
DSDPBeP86	Def2-QZVPPD	ACN	b	+9.8	+7.5
DLPNO-CCSD(T)	Def2-TZVPPD	ACN (CPCM)	b	+14.7	+12.4
DLPNO-CCSD(T)	Def2-QZVPP	ACN (CPCM)	b	+18.2	+16.0

<sup>a</sup> Quasi-harmonic analysis using GoodVibes, with cutoff of 200 cm<sup>-1</sup>. Temp = 40 K. Scale factor = 0.9857.

<sup>b</sup> B3LYP-D3(BJ)/def2-TZVPPD (SMD, acetonitrile) optimized geometry.

**Cartesian coordinates of optimized geometries**  
B3LYP-D3(BJ)/def2-TZVPPD (SMD, acetonitrile)

PhICl <sub>2</sub>	+1,1
0, 1 (charge and multiplicity)	
53        1.131766 -0.000004 -0.000000	53              0.486317 -1.169889 -0.000002
6        -0.975580 0.000006 -0.000001	6              0.934986 0.887802 -0.000003
6        -1.635117 0.143262 1.212082	6              1.067814 1.531011 1.221088
6        -3.025476 0.143532 1.199343	6              1.348856 2.892885 1.208070
6        -3.716031 0.000008 0.000000	6              1.488152 3.568830 0.000005
6        -3.025477 -0.143516 -1.199343	6              1.348828 2.892898 -1.208064
6        -1.635118 -0.143248 -1.212083	6              1.067785 1.531024 -1.221090
1        -1.086864 -0.252499 -2.135994	1              0.958339 0.993744 -2.151135
1        -3.564335 -0.254851 -2.130252	1              1.458814 3.420427 -2.145534
1        -4.797518 0.000007 0.000001	1              1.708132 4.627615 0.000008
1        -3.564333 0.254869 2.130252	17             2.942480 -1.703405 -0.000004
1        -1.086862 0.252515 2.135993	7              -1.695138 -0.496673 0.000004
17        1.123314 -2.541657 0.073063	6              -2.316237 -0.288764 -1.168006
17        1.123340 2.541650 -0.073062	6              -2.316240 -0.288773 1.168012
	6              -3.623884 0.157357 -1.199616
	1              -1.745449 -0.480212 -2.064600
	6              -3.623887 0.157348 1.199623
PhICl <sub>2</sub> Pyr (compound 2)	0,1
0,1	1              -1.745453 -0.480227 2.064605
53        0.000000 -0.000000 0.196272	6              -4.286466 0.385418 0.000003
6        0.000000 -0.000000 2.313853	1              -4.106176 0.321886 -2.151683
6        0.000000 1.216995 2.983585	1              -4.106181 0.321869 2.151690
6        0.000000 1.207588 4.374049	1              -5.308506 0.737247 0.000004
6        0.000000 -0.000000 5.065697	
6        -0.000000 -1.207588 4.374049	PhICl <sup>+</sup>
6        -0.000000 -1.216995 2.983585	+1,1
1        0.000000 -2.148907 2.436713	53             -1.131895 -0.595398 0.016331
1        0.000000 -2.144809 4.913867	6              0.895851 -0.164664 0.004565
1        0.000000 -0.000000 6.147333	6              1.542992 0.001142 1.228007
1        0.000000 2.144809 4.913867	6              2.904067 0.264658 1.205856
1        0.000000 2.148907 2.436713	6              3.579814 0.356192 -0.009126
17        2.549053 -0.000000 0.197059	6              2.907424 0.184290 -1.217191
17        -2.549053 0.000000 0.197059	6              1.546274 -0.079356 -1.225425
7        -0.000000 0.000000 -2.659603	1              1.005888 -0.214001 -2.150318
6        -0.000000 -1.148088 -3.340006	1              3.441788 0.255643 -2.154051
6        0.000000 1.148088 -3.340006	1              4.641035 0.563845 -0.014604
6        -0.000000 -1.196462 -4.727436	1              3.435766 0.399214 2.137310
1        -0.000000 -2.057460 -2.751144	1              1.000296 -0.071276 2.158443
6        0.000000 1.196462 -4.727436	17             -1.987815 1.602888 -0.044850
1        0.000000 2.057460 -2.751144	
6        -0.000000 0.000000 -5.433616	Pyridine
1        -0.000000 -2.149671 -5.236993	0,1
1        0.000000 2.149671 -5.236993	7              0.000000 -0.000000 1.411136
1        -0.000000 0.000000 -6.515320	6              -0.000000 1.143467 0.719344
[PhI(Pyr)Cl] <sup>+</sup>	6              -0.000000 -1.143467 0.719344
	6              -0.000000 1.194428 -0.669087

1	-0.000000	2.058703	1.299784	6	0.000046	3.327779	-1.039519
6	-0.000000	-1.194428	-0.669087	6	0.000042	1.940541	-1.135480
1	-0.000000	-2.058703	1.299784	1	0.000067	1.448126	-2.095931
6	-0.000000	0.000000	-1.377832	1	0.000075	3.921357	-1.943273
1	-0.000000	2.148854	-1.176961	1	0.000012	5.024232	0.271364
1	-0.000000	-2.148854	-1.176961	1	-0.000054	3.667728	2.340307
1	-0.000000	0.000000	-2.459688	1	-0.000058	1.193127	2.199761
				7	2.249772	-0.776310	-0.042667
Phl				6	2.915341	-0.544131	-1.182642
0,1				6	2.893826	-0.958528	1.118644
53	0.000000	1.550968	0.000000	6	4.295107	-0.482127	-1.189778
6	0.000000	-0.564602	-0.000000	1	2.321518	-0.408588	-2.074341
6	0.000000	-1.246551	1.211368	6	4.273299	-0.908268	1.171950
6	0.000000	-2.638410	1.203289	1	2.283776	-1.140248	1.991111
6	0.000000	-3.335937	-0.000000	6	4.983853	-0.666583	0.002873
6	0.000000	-2.638410	-1.203289	1	4.813203	-0.292933	-2.118060
6	0.000000	-1.246551	-1.211368	1	4.773776	-1.056461	2.117168
1	0.000000	-0.706566	-2.147082	1	6.063727	-0.622433	0.020905
1	0.000000	-3.173920	-2.143486	7	-2.249776	-0.776304	-0.042673
1	0.000000	-4.417578	-0.000000	6	-2.893836	-0.958562	1.118628
1	0.000000	-3.173920	2.143486	6	-2.915340	-0.544085	-1.182643
1	0.000000	-0.706566	2.147082	6	-4.273309	-0.908299	1.171930
				1	-2.283791	-1.140314	1.991092
Phl(pyr) <sub>2</sub> <sup>2+</sup>				6	-4.295106	-0.482079	-1.189783
+2,1				1	-2.321513	-0.408514	-2.074335
53	-0.000002	-0.888190	-0.068558	6	-4.983858	-0.666572	0.002858
6	0.000003	1.213713	0.045939	1	-4.773791	-1.056523	2.117141
6	-0.000031	1.795847	1.304182	1	-4.813197	-0.292853	-2.118062
6	-0.000028	3.184806	1.372909	1	-6.063731	-0.622421	0.020887
6	0.000010	3.944732	0.207471				

## 6. References

1. O. V. Dolomanov, L. J. Bourhis, R. J. Gildea, J. A. K. Howard and H. Puschmann, *J. Appl. Cryst.*, 2009, **42**, 339-341.
2. G. M. Sheldrick, *Acta Cryst. A*, 2015, **71**, 3-8.
3. G. M. Sheldrick, *Acta Cryst. C*, 2015, **71**, 3-8.
4. C. J. Setter, J. J. Whittaker, A. J. Brock, K. S. Athukorala Arachchige, J. C. McMurtrie, J. K. Clegg and M. C. Pfrunder, *CrystEngComm*, 2020, **22**, 1687-1690.
5. B. Guillot, L. Viry, R. Guillot, C. Lecomte and C. Jelsch, *J. Appl. Cryst.*, 2001, **34**, 214-223.
6. N. K. Hansen and P. Coppens, *Acta Cryst.*, 1978, **34**, 909-921.
7. F. H. Allen and I. J. Bruno, *Acta Cryst.*, 2010, **66**, 380-386.
8. C. Jelsch, B. Guillot, A. Lagoutte and C. Lecomte, *J. Appl. Cryst.*, 2005, **38**, 38-54.
9. R. Wang, T. S. Dols, C. W. Lehmann and U. Englert, *Chem. Commun.*, 2012, **48**, 6830.
10. R. Wang, C. W. Lehmann and U. Englert, *Acta Cryst.*, 2009, **65**, 600-611.
11. C. Merkens, F. Pan and U. Englert, *CrystEngComm*, 2013, **15**, 8153.
12. M. S. Pavan, R. Pal, K. Nagarajan and T. N. Guru Row, *Cryst. Growth Des.*, 2014, **14**, 5477-5485.
13. A. Wang, R. Wang, I. Kalf, A. Dreier, C. W. Lehmann and U. Englert, *Cryst. Growth Des.*, 2017, **17**, 2357-2364.
14. R. Wang, D. Hartnick and U. Englert, *Z. Kristallogr.*, 2018, **233**, 733-744.
15. R. Wang, I. Kalf and U. Englert, *RSC Advances*, 2018, **8**, 34287-34290.
16. R. Wang, J. George, S. K. Potts, M. Kremer, R. Dronskowski and U. Englert, *Acta Cryst. C*, 2019, **75**, 1190-1201.
17. F. Otte, J. Kleinheider, W. Hiller, R. Wang, U. Englert and C. Strohmann, *J. Am. Chem. Soc.*, 2021, DOI: 10.1021/jacs.1c00239.
18. Gaussian 16 Rev. A.03, 2016
19. A. D. Becke, *J. Chem. Phys.*, 1993, **98**, 5648-5652.
20. C. Lee, W. Yang and R. G. Parr, *Physical Review B*, 1988, **37**, 785-789.
21. S. Grimme, S. Ehrlich and L. Goerigk, *J. Comp. Chem.*, 2011, **32**, 1456-1465.
22. F. Weigend and R. Ahlrichs, *Phys. Chem. Chem. Phys.*, 2005, **7**, 3297.
23. D. Rappoport and F. Furche, *J. Chem. Phys.*, 2010, **133**, 134105.
24. A. V. Marenich, S. V. Jerome, C. J. Cramer and D. G. Truhlar, *J. Chem. Theo. Comp.*, 2012, **8**, 527-541.
25. E. D. Glendening, C. R. Landis and F. Weinhold, *J. Comp. Chem.*, 2013, **34**, 1429-1437.
26. F. Neese, *WIREs Comp. Mol. Sci.*, 2018, **8**, e1327.
27. G. Luchini, J. V. Alegre-Requena, I. Funes-Ardoiz and R. S. Paton, *F1000Research*, 2020, **9**, 291.